Materials Research Proceedings **26** (2023) 429-434 https://doi.org/10.21741/9781644902431-70

Optimal design of single-degree-of-freedom vibro-impact system under harmonic base excitation

Giuseppe Perna[1,a*], Maurizio De Angelis[1,b] and Ugo Andreaus[1,c]

[1] Department of Structural and Geotechnical Engineering, Sapienza University of Rome, Via Eudossiana 18, Rome, 00148, Italy

[a]giuseppe.perna@uniroma1.it, [b]maurizio.deangelis@uniroma1.it, [c]ugo.andreaus@uniroma1.it

Keywords: Vibro-Impact Systems, Dynamic Response Control, Bumper, Gap, Numerical Modeling, Harmonic Base Excitation

Abstract. Strong seismic excitations can induce considerable displacements in base-isolated structures. These may in turn cause damage to the isolation system or impacts against adjacent structures in the event of an insufficient seismic gap. A strategy of reducing displacements can be achieved through the interposition, between the isolated structure and adjacent structures, of deformable and dissipative devices, called bumpers. In this paper, the response of single-degree-of-freedom (SDOF) base-isolated systems subjected to sine excitations and whose displacements are limited by optimally designed bumpers are analyzed, the bumpers being designed according to an optimal design criterion.

Introduction

One of the most widely used strategies for passive control of the dynamic response of sensitive structures and equipment is base isolation. This strategy consists of interposing a highly horizontally deformable element between the base floor and the structure (or equipment), so that the period of the system is increased significantly resulting in a reduction of the transmitted acceleration. However, strong earthquakes can cause large displacements at the isolated floor level, exceeding its limit deformation, or induce impacts with adjacent elements. Rigid impact causes significant increases in acceleration and floor drifts that can cause serious damage to both structural and nonstructural elements [1].

An effective strategy to reduce and control the adverse effects due to large isolation floor displacements is the interposition of deformable and dissipative devices, called bumpers. Various experimental investigations have been conducted by the authors on the influence of bumpers on the dynamic response of single-degree-of-freedom (SDOF) systems subjected to sine base excitation [2-4]. From these studies, it was observed that the parameters governing the impact between system and bumper can be identified by three elements: gap (distance between mass and bumper), stiffness and damping of the bumper. The authors, moreover, based on the experimental investigations defined a numerical model that allowed the identification of optimality relations between bumper stiffness, bumper damping coefficient and gap, reducing the design of such a control strategy to a single parameter [3-7].

This paper analyzes the response obtained from a numerical model of SDOF system constrained by two bumpers, arranged symmetrically on both sides of the mass of the system with an initial gap, subjected to sine excitation. The design of bumpers is done in accordance with the optimality relationship [6] and the optimal design curve [7]. The absolute maximum values of the response in absolute mass acceleration and relative mass displacement are represented as a function of frequency ratio and for six initial gaps. All results shown are represented in dimensionless terms so that they can be generalized.

The text is organized as follows: the first paragraph introduces the model and its equations of motion; the second paragraph explains the optimal design criterion that is used to identify the

Materials Research Proceedings **26** (2023) 429-434 https://doi.org/10.21741/9781644902431-70

parameters governing the impact; the third paragraph reports the results of the numerical analysis; and finally, the fourth paragraph reports the conclusions and possible future developments of the work.

Model and equations of motion

The model adopted in the numerical analyses is shown in Fig. 1. The figure represents a vibro-impact single-degree-of-freedom (SDOF) system that consists of a mass M, a damper D and two deformable and dissipative obstacles, arranged symmetrically on both sides of the mass with an initial gap G_{0j} (j=R right side, j=L left side) and denoted as right bumper B_R and left bumper B_L, respectively. The damper and the bumpers are modeled by a linear elastic element, with stiffness K and K_j *(j=R,L)*, respectively, and a linear viscous dashpot, with damping coefficient C and C_j *(j=R,L)*, respectively, arranged in parallel. The system is subjected by a sine base acceleration $A_t(t) = A_G sin(\Omega t)$, where A_G is the amplitude and Ω in the circular frequency of this excitation. Finally, in figure 1 $u(t)$ refers to the relative displacement of the mass with respect to the ground, and $u_j(t)$ *(j=R,L)* refers to the deformation of the bumper.

The equations of motion were written in dimensionless form to make them as general as possible. The components of the equation were normalized with respect to $F^* = M\omega^2 u^*$, which represents the maximum force in the SDOF system in free flight (without obstacles, FF): the quantity $u^* = u_{st} R_{d,max}$ represents the maximum relative displacement in FF, where $u_{st} = A_G/\omega^2$ is the static displacement and $R_{d,max} = 1/(2\xi\sqrt{1-\xi^2})$ is the maximum value of the dynamic amplification factor $R_d(\xi, \beta)$; while $\omega = \sqrt{K/M}$ denotes the frequency of the system. The frequency ratio $\beta = \Omega/\omega$ and the damping ratio $\xi = C/(2M\omega)$, are introduced and the dimensionless time $\tau = \omega t$ is defined. In the dimensionless equations, the quantities $q = u/u^*$ and $q_j = u_j/u^*$ *(j=R,L)* are the dimensionless displacement of the mass and dimensionless deformation of the bumper, respectively. Similarly, the dimensionless gap is $\delta_{0j} = G_{0j}/u^*$ *(j=R,L)* and can take values comprised within the range $0 \le \delta_{0j} \le 1$. Finally, $f(\tau) = 2\xi q'(\tau) + q(\tau)$ is the damper dimensionless force, $f_j(\tau) = 2\xi\gamma_j q'_j(\tau) + \lambda_j q_j(\tau)$ with (j=R,L) –where $\gamma_j = C_j/C$ and $\lambda_j = K_j/K$– as the dimensionless contact forces, and $a_G = 2\xi\sqrt{1-\xi^2}$ as the dimensionless amplification of the dimensionless sine excitation $a_t(\tau)$.

Thus, the motion equations of the model can be written in the following dimensionless form:

$$\begin{cases} q''(\tau) + f(\tau) + f_j(\tau) \cdot \psi_1[\delta_j(\tau)] \cdot \psi_2[f_j(\tau)] = -a_G sin\beta\tau \\ f_i(\tau) = 0 \end{cases}; \quad (1)$$

where it is assumed that if the mass is in contact with the left bumper, then j=L and i=R, or if the mass is in contact with the right bumper, then j=R and i=L. In the equations the Heaviside functions ψ_1 and ψ_2 are defined as follows:

$$\text{contact} \quad \psi_1[\delta_j(\tau)] = \begin{cases} 0, & \delta_j(\tau) > 0 \\ 1, & \delta_j(\tau) = 0 \end{cases} \quad (j = R, L); \quad (2)$$

$$\text{separation} \quad \psi_2[f_j(\tau)] = \begin{cases} 0, & f_R(\tau) \le 0 \ \ or \ \ f_L(\tau) \ge 0 \\ 1, & f_R(\tau) > 0 \ \ or \ \ f_L(\tau) < 0 \end{cases}; \quad (3)$$

where $\delta_j(\tau)$ *(j=R,L)* represents the gap function in terms of the dimensionless time τ and, if j=R, is equal to $\delta_R(\tau) = \delta_{0R} + q_R(\tau) - q(\tau)$, and, if j=L, is equal to $\delta_L(\tau) = \delta_{0L} - q_L(\tau) + q(\tau)$. In all the equations introduced the apex ($'$) denotes differentiation with respect to the dimensionless time τ.

Because the bumpers are equal and arranged symmetrically on both sides of the mass $\gamma_R = \gamma_L = \gamma$, $\lambda_R = \lambda_L = \lambda$ and $\delta_{0R} = \delta_{0L} = \delta_0$.

Materials Research Proceedings **26** (2023) 429-434 https://doi.org/10.21741/9781644902431-70

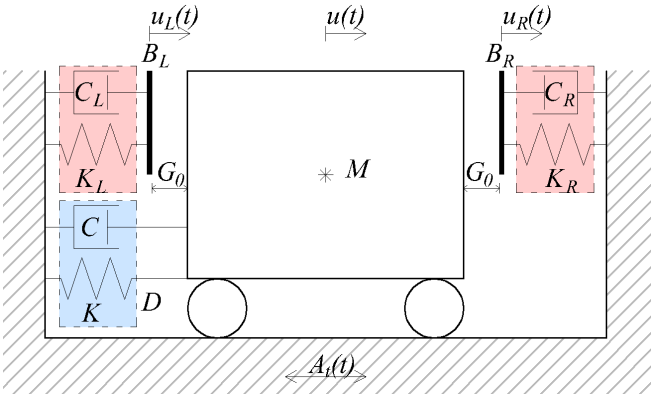

Fig. 1. ***Model of the vibro-impact system.***

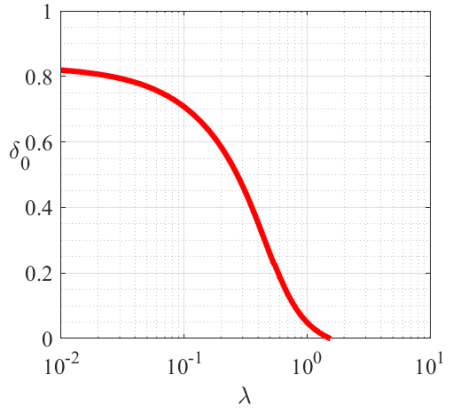

Fig. 2. ***Optimal design curve of the bumper.***

Optimal design of the bumpers

In order to optimize the control of the dynamic response of the system, the physical parameters governing the impact (gap δ_0, stiffness λ and damping γ of the bumper) to be adopted are obtained in relation to an optimal design criterion based on a relationship that links damping ratio ξ of the system with parameters λ and γ of the bumpers [6], and on a curve in which bumper stiffness λ is identified in relation to the gap δ_0 [7].

The optimality relationship is defined as follows:

$$\frac{\gamma}{\lambda} = \frac{1}{2\xi}. \tag{4}$$

This relationship was obtained by a parametric analysis in which, for each investigated δ_0, and for fixed values of ξ and of γ, the value of λ was searched such that the peak acceleration of the mass in the primary resonance is minimized. This is possible because the bumper is fully exploited: the bumper has sufficient time to recover its deformation before the next impact, dissipating all the deformation energy accumulated up to then, and it does not remain inactive because the next impact occurs practically immediately after recovery.

The optimality relationship (4) is independent of the gap and, through this relationship, it is possible to reduce the number of impact parameters from three, which in dimensionless terms can be identified as δ_0, λ and γ, to two, since by choosing λ we obtain the value of the corresponding γ.

With the introduction of the optimal curve an additional constraint is introduced, reducing the bumper design to one parameter, the dimensionless gap δ_0. The optimal design curve, shown in Fig. 2, associates to each δ_0 a pair of values λ and γ (Eq. 4), which minimizes the peak absolute acceleration of the mass in primary resonance and therefore the force acting on the mass.

Looking at the red curve in figure 2, it is clear how the control over the response of vibro-impact system with a dimensionless gap $\delta_0 > 0.82$, is ineffective. This is because, for these values of δ_0, the optimal stiffness ratio λ is so small that the presence of the bumpers is negligible.

Analysis of numerical response

In this paragraph, the numerical responses of the model characterized as follows are analyzed: the damping ratio of the damper is $\xi = 0.10$, the bumper parameters λ and γ are designed in accordance with the optimality relationship (4) and the optimal design curve (Fig.2). The represented response quantities are dimensionless excursion of the absolute acceleration and of the relative displacement, of the mass, both normalized with respect to two different factors:

$$\eta_{a1} = \frac{\Delta\alpha}{\Delta\alpha_0},\ \eta_{a2} = \frac{\Delta\alpha}{\Delta\alpha_t}, \eta_{d1} = \frac{\Delta q}{\Delta q_0},\ \eta_{d2} = \frac{\Delta q}{\Delta q_t}, \tag{5}$$

Materials Research Proceedings **26** (2023) 429-434 https://doi.org/10.21741/9781644902431-70

where $\alpha = a_t + q''$, the dimensionless quantities whit subscript ($_o$) are related to the case of free flight in resonance (FF) and the dimensionless quantities whit subscript ($_t$) are related to the ground. The excursion ($\Delta i, i = \alpha, q$) was calculated as the difference between the maximum and minimum values recorded at steady state of each sub-frequency range.

Figures 3 show the normalized quantities analyzed as a function of the frequency ratio β and in the terms of six dimensionless gaps $\delta_0 = 1, 0.5, 0.3, 0.2, 0.1, 0$, where $\delta_0 = 1$ represents the FF and $\delta_0 = 0$ the case of mass adjacent with bumper.

The curves in Fig. 3a-3b represent the Pseudo-Resonance Curves (PRCs) of the dimensionless absolute acceleration of the mass, normalized in (a) with respect to the FF, and in (b) with respect to the ground. The black curves reproduce dimensionless excursion of the absolute acceleration of the mass in FF, subjected to the dimensionless sine excitation a_t. The curve $\eta_{a1_{FF}}(\beta)$ starts from the value $\eta_{a1_{FF}}(0) \simeq 0.20$ and then attains a peak at resonance, for $\beta = \sqrt{1-2\xi^2} \simeq 0.99$, equal to 1. Once the peak has been passed, for increasing β the acceleration $\eta_{a1_{FF}}$ tends to 0. The curve $\eta_{a2_{FF}}(\beta)$ starts from value 1 ($\beta = 0$), reaches the resonance peak at $\beta = \sqrt{1-2\xi^2} = 5.12$, and, for increasing values of β, $\eta_{a2_{FF}}$ decreases tending to 0 for β tending to infinity. The red dashed curves represented the cases with impact (thinner dashes imply smaller values δ_0). The study of Fig. 3a-3b shows that the curves $\eta_{a1}(\beta)$ are scaled by TR_{max}, that is the maximum value of the resonance transmissibility, relative to curves $\eta_{a2}(\beta)$, so the comments will be unique for both two types of curves, with percentage changes. In Fig. 3a-3b, as δ_0 decreases, a reduction and a shift toward larger β of the acceleration peaks are observed. The lowest value of the peak occurs in the case $\delta_0 = 0$, where a 62% reduction of the maximum acceleration value is obtained with respect to FF. The other cases show a reduction of 48% for $\delta_0 = 0.1$, 30% for $\delta_0 = 0.2$, 22% for $\delta_0 = 0.3$ and 9% for $\delta_0 = 0.5$. The β of resonance increases from 0.99 in the FF to 1.02 for $\delta_0 = 0.5$, 1.09 for $\delta_0 = 0.3$, 1.15 for $\delta_0 = 0.2$, 1.24 for $\delta_0 = 0.1$ up to 1.66 for $\delta_0 = 0$. The dashed curves, for some values of β, overlap with the FF curve: this is because for those values of β and for the value of δ_0 relative to that dashed curve, impact does not occur. The only case in which impact always occurs is the case of mass adjacent to bumpers ($\delta_0 = 0$), which, for $\beta > 1.25$, reports larger accelerations than FF and, for $\beta > 1.52$, larger than the other cases. For the other δ_0 investigated, the acceleration turns out to be greater than FF in a small range of β, between 1.04 and 1.72.

Fig. 3c-3d shows the PRCs of the dimensionless relative displacement of the mass, normalized with respect to FF, in (c), and with respect to the ground, in (d). The black curves represent the dimensionless excursion of the relative displacement of the mass in FF, subjected to the dimensionless sine excitation a_t. The dimensionless displacement curve in FF $\eta_{d1_{FF}}(\beta)$, reports the maximum at $\beta = \sqrt{1-2\xi^2} \simeq 0.99$, in which it takes value 1. For β between 0, in which $\eta_{d1_{FF}}(0) \simeq 0.20$, and $\sqrt{1-2\xi^2}$, $\eta_{d1_{FF}}$ grows as β increases. Passing the peak value, for increasing β the displacement $\eta_{d1_{FF}}$ decreases, tending, in the limit, to the value 0. The dimensionless displacement in FF, $\eta_{d2_{FF}}(\beta)$, reports the maximum in $\beta = 1/\sqrt{1-2\xi^2} \simeq 1.01$ of intensity equal to 5.03. In the first range between 0 and β relative to the maximum, $\eta_{d2_{FF}}$ has an increasing monotonic trend, after which, as β increases, it decreases tending, for infinite β, to the value 1 (maximum ground displacement). In contrast to $\eta_{d1_{FF}}$, $\eta_{d2_{FF}}$ at $\beta = 0$ assuming zero value.

The red dashed curves show the displacement responses of the impacted cases (thinner dashes imply smaller values of δ_0). Referring to Fig. 3c, the peaks of displacements, as δ_0 decreases, move toward larger β and decrease. With respect to FF ($\delta_0 = 1$), η_{d1} decreases by 90% for $\delta_0 = 0$, by 69% for $\delta_0 = 0.1$, by 55% for $\delta_0 = 0.2$, by 42% for $\delta_0 = 0.3$, and by 22% for $\delta_0 = 0.5$, while the β relative to these maximum values turns out to be 1.59, 1.19, 1.13, 1.09, and 1.03,

Materials Research Proceedings **26** (2023) 429-434 https://doi.org/10.21741/9781644902431-70

respectively. Each curve related to $\delta_0 \geq 2\,\xi\sqrt{1-\xi^2}$ ($\simeq 0.2$) is initially coincident with the FF case, until η_{d1}, growing, reaches the value δ_0, causing the impact to occur because the displacement in FF is greater than the gap. Conversely, once the value of β has been exceeded beyond which $\eta_{d1_{FF}} \leq \delta_0$, the curve for that value of δ_0 turns out to coincide with the FF case. The only curve that shows a single point of coincidence with free flight is the one related to $\delta_0 = 0$, for $\beta = 1.75$; this curve also, for $\beta < 1.75$, shows smaller values than for FF, while for $\beta > 1.75$ larger values, with a maximum increase of 28% in displacement value in FF case. The PRCs for the other values of $\delta_0 > 0$ exhibit larger values than FF for $1.27 < \beta < 1.72$ with $\delta_0 = 0.1$, for $1.18 < \beta < 1.40$ with $\delta_0 = 0.2$, for $1.13 < \beta < 1.27$ with $\delta_0 = 0.3$, and for $1.07 < \beta < 1.15$ with $\delta_0 = 0.5$ with maximum increases of 33% (for $\beta = 1.5$), 24% (for $\beta = 1.3$), 18% (for $\beta = 1.2$), and 7% (for $\beta = 1.12$). In Fig. 3c, as δ_0 decreases, there is, as in Fig. 3d, a shift to the right and a reduction of peak displacement whit respect to FF, but at different dimensionless frequencies β and with different percentage reduction: for $\delta_0 = 0$ the peak is for $\beta = 2.04$ with 68% reduction, for $\delta_0 = 0.1$ the peak is for $\beta = 1.35$ with 50% reduction, for $\delta_0 = 0.2$ the peak is for $\beta = 1.22$ with 38% reduction, for $\delta_0 = 0.3$ the peak is for $\beta = 1.15$ with 28% reduction, and for $\delta_0 = 0.5$ the peak is for $\beta = 1.07$ with 13% reduction. As observed in Fig. 3c-3d, the response for $\delta_0 = 0$ never coincides with the FF curve except at $\beta = 1.75$.

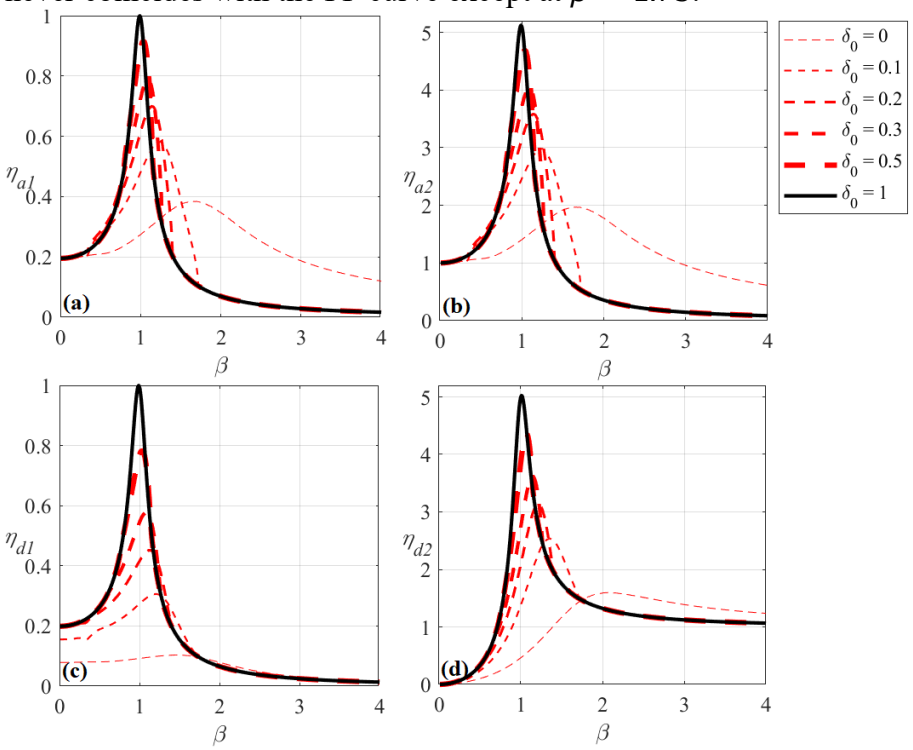

Fig. 3. PRCs of dimensionless acceleration: (a) PRC of $\eta_{a1}(\beta)$; (b) PRC of $\eta_{a2}(\beta)$; and PRCs of dimensionless displacement: (c) PRC of $\eta_{d1}(\beta)$; (d) PRC of $\eta_{d2}(\beta)$. The curves are related to different values of δ_0: in black δ_0=1 (FF), in dashed red δ_0=0.5, 0.3, 0.2, 0.1, 0 (lower thicknesses represent lower δ_0).

Conclusions and future developments

In this paper, the numerical dynamic response of the SDOF system, subjected to sine excitation, constrained by two symmetrically arranged deformable and dissipative bumpers designed with optimality relation (4) and optimal design curve (Fig. 2) is analyzed. Six different values of the design parameter δ_0 (dimensionless gap) are considered: two extreme cases, $\delta_0 = 1$, a touching condition between mass and bumpers representative of FF, and $\delta_0 = 0$, a condition with mass adjacent to the bumpers; and intermediate cases, $\delta_0 = 0.5$, $\delta_0 = 0.3$, $\delta_0 = 0.2$ and $\delta_0 = 0.1$.

The response quantities which have been analyzed are the absolute acceleration of the mass and the relative displacement of the mass with respect to the ground, normalized with respect to both (i) the peak values of acceleration and displacement in FF, and (ii) the peak values of base

acceleration and ground displacement. It was found that as δ_0 decreases, the maximum values of peak acceleration and displacement undergo greater reductions with respect to FF, reporting in the case $\delta_0 = 0$ the greatest reductions (peak of acceleration reduced by 62% for both $\eta_{a1}(\beta)$ and $\eta_{a2}(\beta)$, peak of displacement reduced by 90% for $\eta_{d1}(\beta)$, and by 68% for $\eta_{d2}(\beta)$). However, the case $\delta_0 = 0$ reports larger values of acceleration for $\beta > 1.52$, compared with the other cases examined. A phenomenon of increased displacement, due to the presence of bumper, was also observed for some β following the primary resonance in FF ($1.08 < \beta < 1.15$ for $\delta_0 = 0.5$, $1.13 < \beta < 1.27$ for $\delta_0 = 0.3$, $1.18 < \beta < 1.4$ for $\delta_0 = 0.2$, $1.27 < \beta < 1.71$ for $\delta_0 = 0.1$, $\beta > 1.72$ for $\delta_0 = 0$). This phenomenon is named bouncing-effect in the literature.

These results show that the adoption of this optimal design criterion and an appropriate choice of the gap parameter δ_0 allow beneficial effects in mitigating the dynamic response to be gained. Thus, the need emerges to extend this study to cases of real dynamic actions, such as earthquakes, and evaluate the effects of appropriately designed dissipative and deformable bumpers on systems subjected to different seismic excitations.

References

[1] P.C. Polycarpou, P. Komodromos, On poundings of a seismically isolated building with adjacent structures during strong earthquakes, Earthq. Eng. Struct. Dyn. 39 (2010). https://doi.org/10.1002/eqe.975

[2] U. Andreaus, M. De Angelis, Influence of the characteristics of isolation and mitigation devices on the response of single-degree-of-freedom vibro-impact systems with two-sided bumpers and gaps via shaking table test, Struct. Control Health Monit. 27(2020). https://doi.org/10.1002/stc.2517

[3] G. Stefani, M. De Angelis, U. Andreaus, Scenarios in the experimental response of a vibro impact single-degree-of freedom systems and numerical simulations, Nonlinear Dyn. 103 (2021). https://doi.org/10.1007/s11071-020-05791-4

[4] G. Stefani, M. De Angelis, U. Andreaus, Influence of the gap size on the response of a single-degree-of-freedom vibro-impact system with two-sided constraints: Experimental tests and numerical modeling, Int. J. Mech. Sci. 206 (2021). https://doi.org/10.1016/j.ijmecsci.2021.106617

[5] G. Stefani, M. De Angelis, U. Andreaus, Numerical study on the response scenarios in a vibro-impact single-degree-of-freedom oscillator with two unilateral dissipative and deformable constraints, Commun. Nonlinear Sci. Numer. Simul. 99 (2021). https://doi.org/10.1016/j.cnsns.2021.105818

[6] G. Stefani, M. De Angelis, U. Andreaus, The effect of the presence of obstacles on the dynamic response of single-degree-of-freedom systems: Study of the scenarios aimed at vibration control, J. Sound Vib. 531 (2022). https://doi.org/10.1016/j.jsv.2022.116949

[7] G. Stefani, M. De Angelis, U. Andreaus, Exploit the study of the scenarios for the control of the response of single-degree-of-freedom systems with bumpers, Submitted to Eng. Struct. (2022).